

RESEARCH

Open Access



Single-cell transcriptomics identify a chemotherapy-resistance related cluster overexpressed CLIC3 in ovarian cancer

Zhefeng Li¹, Jie Li^{1,2}, Yue Li¹, Junjie Yi¹, Xiaoting Zhao^{1*} and Wentao Yue^{1*}

*Correspondence:

Xiaoting Zhao
zhao_xiaoting@ccmu.edu.cn
Wentao Yue
yuewt@ccmu.edu.cn

¹Central Laboratory, Beijing Obstetrics and Gynecology Hospital, Capital Medical University, Beijing Maternal and Child Health Care Hospital, Beijing 100026, China
²Department of Clinical Laboratory Diagnostics, Beijing Friendship Hospital, Capital Medical University, Beijing 100054, China

Abstract

Background Chemoresistance, the primary cause of mortality among ovarian cancer (OC) patients, is a multifaceted process encompassing numerous biological phenomena. As sequencing technology continues to advance, single-cell sequencing has surfaced as a potent strategy to elucidate the pathogenesis of OC.

Methods We examined single-cell sequencing data derived from five OC samples (three resistant and two sensitive) and identified an epithelial subcluster associated with chemotherapy resistance and poor prognosis. Using GSVA and cell communication analysis, we explored the unique biological functions and communication characteristics of this resistant subcluster. We performed high dimensional weighted gene co-expression network analysis and differential expression analysis to identify the hub genes of c3. Lastly, we investigated the correlation between the hub gene, CLIC3, and chemotherapy drug sensitivity. We also validated their involvement in specific pathways using TCGA data. The effects and primary mechanism to chemoresistance of CLIC3 was explored.

Results We identified a cell subcluster, denoted as c3, strongly linked to chemoresistance and poor prognosis in OC. This subcluster demonstrated a correlation with both extracellular matrix (ECM) formation and angiogenesis signature, with CLIC3 identified as its key marker. The expression levels of CLIC3 exhibit a significant association with the sensitivity to various chemotherapeutic drugs in OC. Mechanistically, CLIC3 increases OC resistance to cisplatin by promoting integrin $\beta 1$ redistribution and PI3K-AKT pathway.

Conclusions This study offers a novel insight into the progression and chemoresistance of OC. Additionally, we identified a specific cell cluster highly associated with chemoresistance. The marker for this cluster, CLIC3, increases OC resistance to cisplatin by promoting integrin $\beta 1$ redistribution and PI3K-AKT pathway and holds significant potential as a new therapeutic target for OC.

Keywords Ovarian cancer, Chemoresistance, Single-cell transcriptomics, CLIC3, Integrin $\beta 1$, PI3K-AKT pathways



1 Introduction

Ovarian cancer (OC) ranks among the top three malignancies in incidence and mortality within the female reproductive system, posing a significant global healthcare burden [1]. Although platinum-based chemotherapy has significantly improved patient outcomes over the decades, unfortunately, approximately two-thirds of the patients develop resistance to platinum, substantially increasing the five-year mortality rate [2]. Therefore, overcoming chemotherapy resistance in OC patients is an urgent challenge.

Recent years have seen a surge in research into the mechanisms of chemotherapy resistance in OC, with primary focus on drug efflux and the activation of DNA repair pathways [3]. However, emerging studies show that various cancer therapies induce ECM remodeling, resulting in therapy resistance and tumor progression. The major mechanism of ECM-induced resistance is via the interaction with integrins overexpressed by cancer cells [4]. For example, stiffened ECM interacts with β 1-integrin that activates the downstream ILK/PI3K/AKT pathway in cancer cells, thereby inducing stemness [5].

CLIC3, a member of the Chloride Intracellular Channel (CLIC) family, was initially named for its role in mediating chloride conductance [6]. CLIC3 is overexpressed in bladder cancer and correlates with poor clinical prognosis in patients [7]. Meanwhile CLIC3 promotes pancreatic cancer metastasis and renal cell carcinoma chemoresistance via integrin recycling and membrane redistribution [8, 9]. However, the role of CLIC3 in OC chemoresistance remains undetermined.

In this study, we analyzed single-cell sequencing data from five OC samples and identified a subcluster closely associated with chemotherapy resistance and poor prognosis. Analyses of functionality and cell communication disclosed that this subcluster extensively interacts with the tumor microenvironment, playing a pivotal role in ECM regulation. Building upon this, we identified an overexpressed gene, CLIC3, previously unreported in OC. Then, we explored the correlation between the expression of CLIC3 and chemoresistance with Genomics of Drug Sensitivity in Cancer (GDSC) and The Cancer Genome Atlas Program (TCGA) datasets, which suggested a significant association between CLIC3 and both poor prognosis and chemoresistance. Finally, we found CLIC3 actively participates in pathways related to ECM formation and integrin regulation, which may be the key mechanisms through which it contributes to chemoresistance. In conclusion, our research furthers the exploration of mechanisms underlying OC chemoresistance and introduces a potential new treatment target for OC.

2 Materials and methods

2.1 Public data sources

Public scRNA-seq datasets, with accession numbers GSE154600 and GSE30161, were obtained from the Gene Expression Omnibus database [10] (Additional file 5: Table S1). Additionally, the bulk RNA-seq expression and phenotype datasets for TCGA OC were sourced from UCSC Xena [11].

2.2 Quality control and data integration

scRNA-seq data were processed and analyzed using the Seurat (v 4.1.1) R package. The gene-cell matrix was generated and analyzed using the Seurat software. Additional quality control measures were implemented on the cells: filtering was based on detected genes (range: 300-6000), mitochondrial gene percentage (0-25%), hemoglobin gene

percentage (0-1%), and ribosomal gene percentage (range: 3-80%). Genes expressed in fewer than 5 cells were also eliminated. Uniform Manifold Approximation and Projection (UMAP) was constructed using principal components. Canonical Correlation Analysis (CCA) via the Seurat package was applied to eliminate batch effects and perform major clustering. Cell types were defined based on biomarker expression.

2.3 Gene set functional analysis

The gene set functional analyses were conducted with R package 'clusterProfiler' [12] and 'GSVA' [13]. GSVA analyses utilized the Gene Ontology (GO), Kyoto Encyclopedia of Genes and Genomes (KEGG), and Reactome pathway databases. The Reactome gene sets were sourced from the 'msigdb' R package.

2.4 Survival analysis

The most significant marker genes from each cell subcluster were identified. Then, using GSVA, feature scores for the subclusters of the 418 OC patients in the TCGA cohort were computed. Incorporating the overall survival time, a Kaplan–Meier survival analysis was conducted using the 'survival' R package.

Cox survival analysis was performed using KM-Plotter online database for OC microarray (<https://kmplot.com/>). For the KM-Plotter analysis, only the best probe sets from JetSet were utilized. The performance-based thresholds, which serve as cut-offs, were automatically selected for the percentiles of subjects in both low and high gene-expression groups.

2.5 Identification of chemo-resistant clusters

The Scissor R package represents a novel approach. It leverages phenotype data—including disease stage, tumor metastasis, treatment response, and survival outcomes—gathered from bulk assays to discern cell subpopulations most strongly associated with these phenotypes in single-cell data [14]. In our study, we employed three data sources as inputs for the Scissor algorithm: (1) A single-cell expression matrix of OC. (2) A bulk expression matrix of OC sourced from the TCGA database. (3) The aforementioned clinical data on chemotherapy response in OC patients from the TCGA database. The Scissors algorithm leverages differential gene expression profiles of OC cases with divergent chemotherapy responses from the TCGA database to classify cells into three subsets based on epithelial transcriptomic signatures: background cells, Scissors+ cells (chemo-resistant cells), and Scissors- cells (chemo-sensitive cells).

2.6 Cell–cell communication analysis

We used R package 'CellChat' (CellChat v1.1.3) to perform cell–cell communication analysis [15]. Cellchat database including 'Secreted Signaling', 'ECM-Receptor' and 'Cell–Cell Contact' were used.

2.7 HdWGCNA analysis

The R package 'hdWGCNA' was utilized to perform high-dimensional weighted gene co-expression network analysis (hdWGCNA), thereby constructing a scale-free network at the single-cell level. With a threshold set for scale-free topology model fit at > 0.85 , a

soft threshold of 9 was chosen for optimal connectivity. The TCGA cohort was subsequently scored using GSEA, in relation to modules.

2.8 Differential expression analysis

We conducted differential expression analysis on 367 scissor+ cells and 703 scissor- cells by R package 'limma'. Genes with $\log_2\text{FoldChange} > 1$ and adjusted p value < 0.05 were regarded as differential expressed genes (DEGs).

2.9 Drug sensitivity prediction

Using the R package 'oncoPredict', we conducted a prediction analysis of drug sensitivity for commonly used and potential chemotherapy drugs in OC treatment. TCGA cohort including 418 patients was divided into two groups by the median of CLIC3 mRNA expression.

2.10 Cell culture and small interfering RNA (siRNA) transfection

Human OC cell lines SKOV3 was cultured using previously established protocols [16]. After the cell lines reached a confluency of 50–60%, they were transfected with 50 pmol/mL of siRNAs using lipofectamine 3000 (Invitrogen, Carlsbad, CA, USA) for 6 h. Then, the transfection system was removed and cells were cultured under standard culture conditions. Protein analysis and functional experiments were performed digested cells 48 h after seeding. The siRNAs against CLIC3 were obtained from Sangon Biotech. (Shanghai, China) and the sequences of siRNA were as follows: si1 (sense: 5'-AGCUCC AGCUGUUUGUCA-3'), si2 (sense: 5'-AGUUCUCCGCGUUCAUCA-3').

2.11 Western blot and antibodies

Western blot was conducted following established procedures described in previous studies [17]. Then were incubated with primary antibodies at 4 °C overnight, as following dilutions: anti-CLIC3 (1:1000, 15971-1-AP, Proteintech), anti-PI3K (1:1000, 4249, CST), anti-pAKT (1:1000, 9018, CST), anti-AKT(1:1000, 2938, CST), anti-GAPDH (1:3000, ab9482, Abcam). Next, the membranes were incubated with horseradish peroxidase-conjugated rabbit IgG secondary antibodies (1:3000, abcam) for 1 h at room temperature. The expression levels were detected by ECL kit (Roche Diagnostics, Basel, Switzerland) using WB imaging system (Bio-Rad, California, America).

2.12 Spheroid formation assay

Spheroid formation assays were performed under serum-free, nonadherent culture conditions. The cells were seeded at a density of 100 cells per well in 6-well low-adhesion plates containing serum-free DMEM supplemented with dual antibiotics (penicillin/streptomycin). Cisplatin was administered to the culture medium at a final concentration of 10 $\mu\text{g/mL}$ 24 h post-seeding. Following a 14-day incubation period, spheroids with diameters exceeding 100 μm were quantified using bright-field microscopy.

2.13 Cell proliferation assay

For drug sensitivity assays, cells (3000 cells per well) were plated on 96-well plates overnight and subsequently treated with specified concentrations of cisplatin. After 72 h of cisplatin exposure, cytotoxicity was evaluated using the Cell Counting Kit-8.

2.14 Immunofluorescence staining

Briefly, cells on glass coverslips were washed with phosphate-buffered saline (PBS), fixed with 4% paraformaldehyde, and permeabilized with 0.5% Triton X-100. Cells were then blocked with 1% bovine serum albumin and incubated overnight at 4 °C with the primary antibody. Next, cells were incubated with DAPI and secondary antibodies. Finally, cell membrane staining was performed in accordance with the manufacturer's protocol. Images were captured using a Leica Mica microscope.

2.15 Statistical analysis

All experiments were independently repeated at least three times, and statistical differences between experimental groups were assessed using Student's t-test or ANOVA analysis. GraphPad Prism 8.0.2 software and R 4.1.2 was employed for statistical analysis. Statistical significance was denoted as $*p < 0.05$, $**p < 0.01$, and $***p < 0.001$.

3 Result

3.1 Single-cell landscape of platinum resistant and platinum sensitive tissues in HGSOc

We conducted single-cell RNA sequencing (scRNA-seq) on three platinum-resistant and two platinum-sensitive HGSOc tissues, generating a dataset of 50,006 cells. After setting the number of principal components (nPCs) to 30 and the resolution to 1, we utilized the Uniform Manifold Approximation and Projection (UMAP) method for non-linear dimension reduction, identifying 26 cell clusters (Additional file 1: Fig. S1). Utilizing canonical markers, we successfully distinguished six cell types (Fig. 1A, B: B cells (markers: CD79A, CD79B), endothelial cells (markers: VWF, CLDN5), epithelial cells (markers: PAX8, CD24, EPCAM, KRT19), fibroblasts (markers: COL1A1, DCN), myeloid cells (markers: FCER1G, CD14, CD68) and T cells (markers: CD3D, CD3E, TRAC) (Fig. 1C). As chemotherapy resistance increased, we observed a decrease in the composition of immune cells, and a relative increase in the composition of epithelial cells (Fig. 1D). This suggests that the increase in malignant epithelial cells and the initiation of immune evasion may be key mechanisms by which OC acquires chemotherapy resistance. Based on the above findings, we next extract the epithelial cell and recluster into seven subclusters named c1 to c7 based on gene expression similarity for in-depth exploration of key resistant subclusters (Fig. 1E). Firstly, we examined the origins of each subcluster. The results indicated that most subclusters predominantly originated from resistant samples, with subclusters c1, c3, c4, and c7 being particularly prominent. In contrast, subcluster c2 primarily derived from sensitive samples (Fig. 1F). Of note, gene expression profiles of these subclusters were markedly different (Fig. 1G). To elucidate the functions within the subclusters, we conducted a gene set variation analysis (GSVA) and AUCell analysis. The findings revealed that various biological processes were linked with distinct cancer subclusters (Fig. 1H, Additional file 2: Fig. S2). C1, c2 and c5 enriched metabolic related pathways such as "phosphagen metabolic process," "regulation of long chain fatty acid import into cell" and "succinate metabolic process". C3 demonstrated an invasive signature, characterized by malignant biological properties such as epithelial-mesenchymal transition, extracellular matrix, angiogenesis and autophagy, which were previously thought to be associated with both angiogenesis and resistance to chemotherapy. C4 enriched cell cycle and DNA repair pathway such as "negative regulation of G0 to G1 transition," while c6 enriched immunity related pathways such as "interleukin 2 mediated

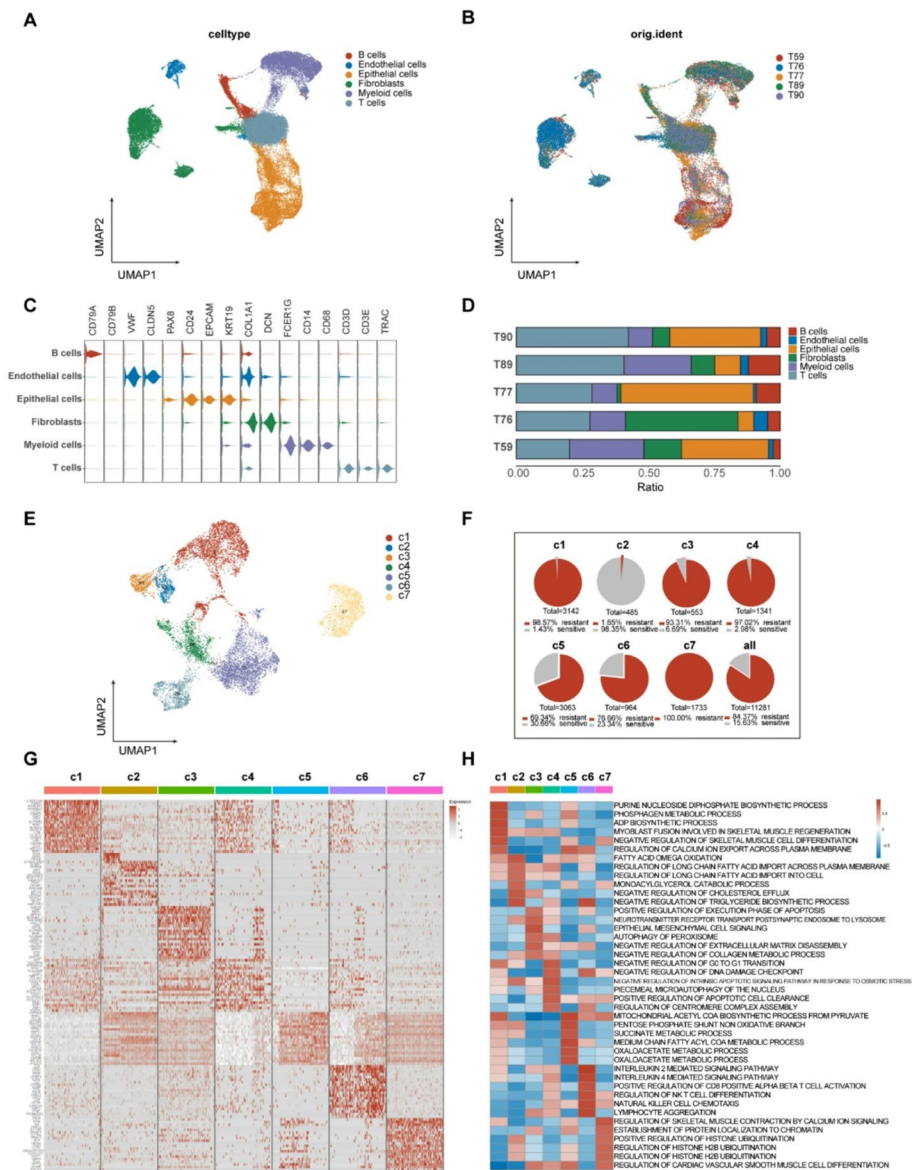


Fig. 1 Single-cell atlas of 5 patients. A, B UMAP of the all 50,006 cells. Colored by cell type or patient. (Chemotherapy resistant: T59, T76, T77; chemotherapy sensitive: T89, T90). C The violin plot illustrated the markers for each cell type. D The bar plot depicted the distribution of cell proportions among patients. E UMAP of the all 11,281 epithelial cells. Colored by cell type. F Pie chart showing the sample origin of each subclusters. G The top 20 genes for each epithelial cell subclusters. H GO pathways of epithelial cell subclusters determined by GSVA

signaling pathway” and “regulation NK T cell differentiation”. Thus, functional analysis revealed that c3 and c4 were chemotherapy resistant associated subclusters. Studying these subclusters may help us understand the mechanism of OC resistant.

3.2 Identification of c3 as a resistant subcluster in epithelial cells

To further determine the key-clusters that lead to chemotherapy resistance, we utilized bulk RNA-seq and clinical data from The Cancer Genome Atlas (TCGA) to explore the association between subclusters and both patient prognosis and chemotherapy sensitivity. Of the seven identified subclusters, only two showed a significant correlation with prognosis. Specifically, subcluster c3 was negatively correlated with overall survival (OS)

time (log-rank test, $p=0.039$), whereas subcluster c6 exhibited a positive correlation with OS time (log-rank test, $p=0.0075$) (Fig. 2A, Additional file 3: Fig. S3). The analysis of biological processes suggested that c6 is an immune-activated subcluster, which is consistent with its association with a better prognosis. Subsequently, we investigated the correlation between each subclusters and chemotherapy sensitivity in OC patients. The results showed that only the c3 was significantly associated with chemoresistance (Fig. 2B, C). We next conducted independent validation in another Gene Expression Omnibus database (GSE30161), which similarly demonstrated that only the c3 was associated with both poor prognosis (log-rank test, $p=0.047$) and chemoresistance in OC patients (Fig. 2D, E, Additional file 4: Fig. S4). The above study demonstrated a strong association between c3 and chemotherapy resistance in ovarian OC two independent cohorts. To mitigate the impact of cell clustering on chemotherapy resistance, the

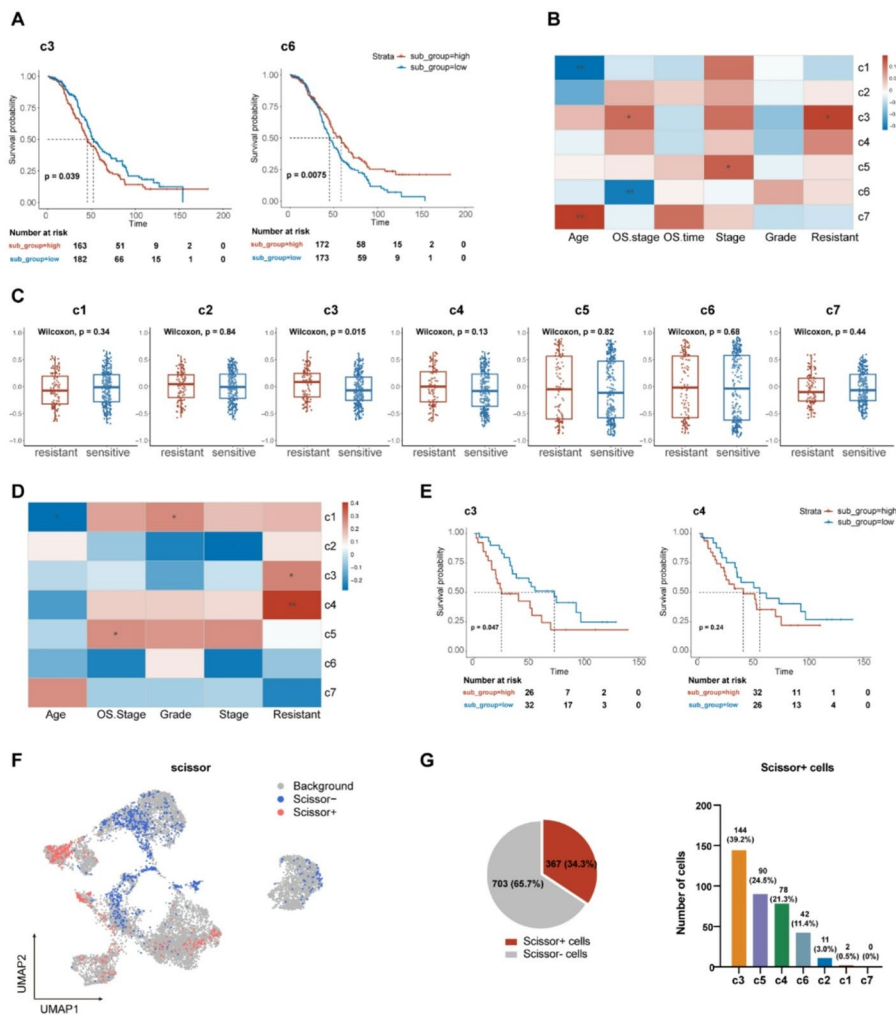


Fig. 2 Identified an epithelial subcluster, c3, associated with chemotherapy resistance and poor prognosis in OC. A Kaplan–Meier analysis for patients in TCGA cohort with high and low GSVA score based on the top markers of c3 (left) and c6 (right). B The heatmap illustrated the correlations between subclusters and clinical phenotypes within the TCGA cohort. C Box plot showed each subclusters score between chemo-sensitive and chemo-resistant OC patients in TCGA cohorts. D The heatmap illustrated the correlations between subclusters and clinical phenotypes within the GSE30161 cohort. E Kaplan–Meier analysis for patients from GSE30161 cohort with high and low GSVA score based on the top markers of c3 (left) and c4 (right). F Scissor algorithm identifying chemo-resistant and sensitive epithelial phenotypes in OC (scissor-: chemo-sensitive cells; scissor+: chemo-resistant cells). G Pie plot and box plot showed the subclusters distribution of scissors + cells

Scissor algorithm, which is a novel approach that utilizes the phenotypes, such as disease stage, tumor metastasis, treatment response, and survival outcomes, was applied to selectively identify cisplatin-resistant epithelial cells. Ultimately, we identified 703 scissor- cells (chemo-sensitive cells) and 367 scissor+ cells (chemo-resistant cells). Source analysis of the scissor+ cells revealed that c3 was the largest contributor, accounting for approximately 39.2% of the total (Fig. 2E, G). In this section, we pinpointed a specific OC cell subcluster, c3, that showed a connection with chemoresistance and a poorer prognosis.

3.3 C3 enhances tumor chemoresistance by facilitating cell-to-cell communication with mesenchymal cells

We conducted a cell-to-cell communication analysis to clarify the interactions between different subclusters and the TME cells. The results indicated that c3 had the most interactions with mesenchymal cells (including vascular endothelial cells and fibroblasts), suggesting that c3 may promote angiogenesis, formation of the extracellular matrix (ECM) and chemoresistance through cellular communication with mesenchymal cells (Fig. 3A, B). Specifically, we found that c3 played a dominant role in cell communication within these signaling pathways related to formation of the ECM, including Collagen, Laminin and FN1 (Fig. 3C, D, E). Additionally, the interaction of the VEGF pathway, primarily with endothelial cells, was significantly stronger in subcluster c3 than in the other six subclusters (Fig. 3F). Further analysis of receptor-ligand roles in the pathways indicated that c3 primarily participates in receiving signals and regulating the formation of the extracellular matrix (Fig. 3G, H, I). C3 acts as a sender in the biological processes where endothelial cells promote angiogenesis (Fig. 3J). We further identified the receptor-ligand interactions within these pathways (Fig. 3K, L). C3 significantly over-expressed the collagen and integrin family genes, which were considered correlating to ECM remodeling and chemoresistance [18]. Moreover, we observed that subcluster c3 expressed higher levels of VEGFA and VEGFB. Concurrently, its receptors - FLT1, PGF, and KDR - were specifically expressed in endothelial cells. This suggests that c3 is a subcluster that promotes angiogenesis. In summary, our work indicated that c3 is a subcluster closely interacting with the TME, potentially enhancing chemotherapy resistance by promoting ECM formation and angiogenesis.

3.4 HdWGCNA identifies the hub genes of c3

Subsequently, we utilized high dimensional weighted gene co-expression network analysis (hdWGCNA) to discern the primary molecular features of c3. Setting a soft threshold of 9, we constructed a scale-free network for c3 to ensure optimal connectivity. This process led to the identification of 10 gene modules (Fig. 4A, B, C). Among the 10 gene modules, only Epi7 ($p = 0.015$) exhibited a significant negative correlation with progression-free survival (PFS) in OC (Fig. 4D). In addition, scores for Epi7 were significantly higher in chemo-resistant patients compared to chemo-sensitive ones, particularly in patients T59 and T60 (Fig. 4E). Therefore, we hypothesized that Epi7 were hub genes responsible for the c3 subcluster's acquisition of chemoresistance. Then we performed GO and KEGG enrichment analyses for Epi7, the functions mainly focused on cell proliferation, cell cycle, and apoptosis related pathways, including 'positive regulation of cell population proliferation', 'regulation of cell cycle' and 'negative regulation of apoptotic

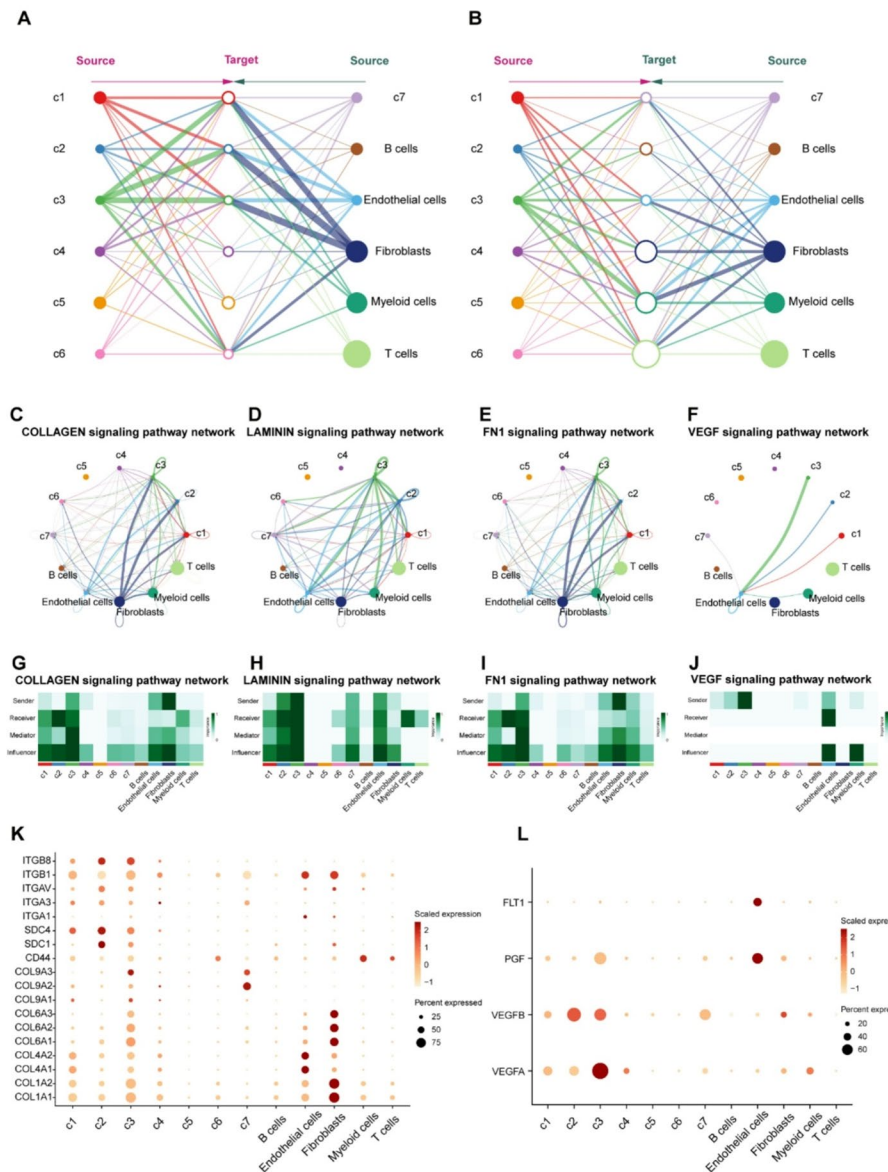


Fig. 3 Cell-to-cell Communications between OC and TME cells. A, B Cell communications among epithelial cells subclusters and TME. The line thickness represents the number of signals targeting either epithelial cells or TME cells. C–F Circle plots showed the interactions of Collagen, Laminin, FN1 and VEGF pathways. G–J Heatmap demonstrating the roles of various subclusters within the pathways. K, L Bubble plots showing the ligands and receptors of Collagen and VEGF pathways

process’ (Fig. 4E, G). It is well known that these pathways play a crucial role in chemotherapy resistance. In conclusion, we investigated the gene expression modules in c3 and pinpointed the hub genes that contribute to chemoresistance.

3.5 CLIC3 is key gene in c3 and associated with chemoresistance

Through differential expression analysis (DEA) of scissor- and scissor+ cells, we discerned 149 genes that were upregulated and 628 genes that were downregulated in scissor+ cancer cells (Fig. 5A, Additional file 6: Table S2). Gene set enrichment analysis (GSEA) results showed that extracellular matrix and integrin-related pathways were significantly upregulated in scissor+ cells (Fig. 5B). This result is consistent with the

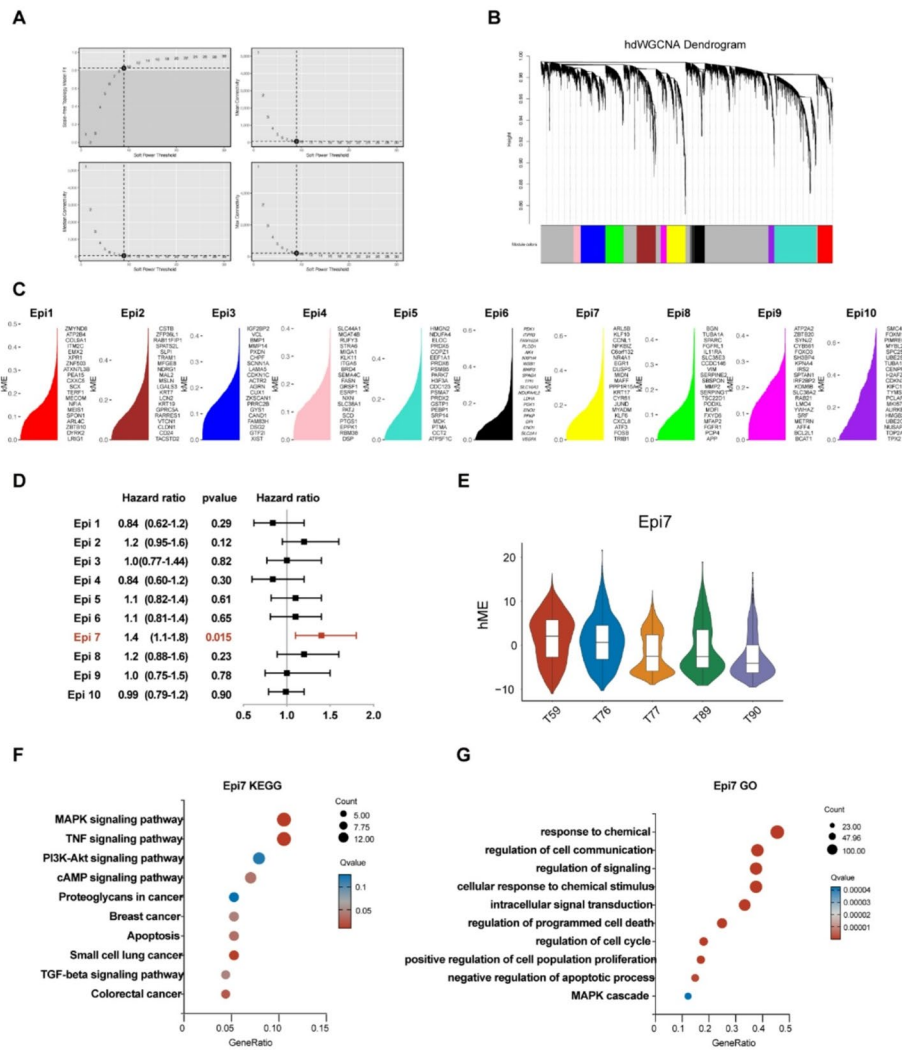


Fig. 4 Identification of gene co-expression modules in OC cells. A, B Weighed gene co-expression network analysis was constructed in malignant cells. C The top 20 eigengenes of each module, ranked by eigengene-based connectivity (kME). D Forest plot demonstrates the association between Epi 1–10 and progression-free survival (PFS) in OC. E Violin plot showed the expression levels of Epi7 across different samples. F, G Dot plot of the KEGG (F) and GO (G) functional enrichment analysis of the module Epi7. (* $p < 0.05$, ** $p < 0.01$, *** $p < 0.001$ in a spearman test.)

biological processes and cell communication findings enriched in the c3. Taking the intersection with the hub genes of Epi7 and c3 Top genes, we obtained 2 genes, HTRA1 and CLIC3 (Fig. 5C). We conducted a functional analysis of these two genes and found that HTRA1 is a secreted enzyme that is proposed to regulate the availability of insulin-like growth factors (IGFs), while CLIC3 is a member of the p64 family and promotes formation of ECM and angiogenesis by regulating integrins. Since CLIC3 aligns more closely with the biological functions and cell communication pathways of c3, we selected it as the focus for subsequent chemoresistance studies. High CLIC3 expression demonstrated a significant negative correlation with PFS in GSE9891 ($p = 0.005$), GSE14764 ($p = 0.049$), GSE26193 ($p = 0.001$) and GSE30161 ($p = 0.002$). Meanwhile, CLIC3 was found to be negatively associated with PFS in the entire sample set ($p = 0.025$) (Fig. 5D). Subsequently, we examined the expression levels of CLIC3 across various epithelial sub-clusters and found that it was specifically expressed in c3, which had previously been

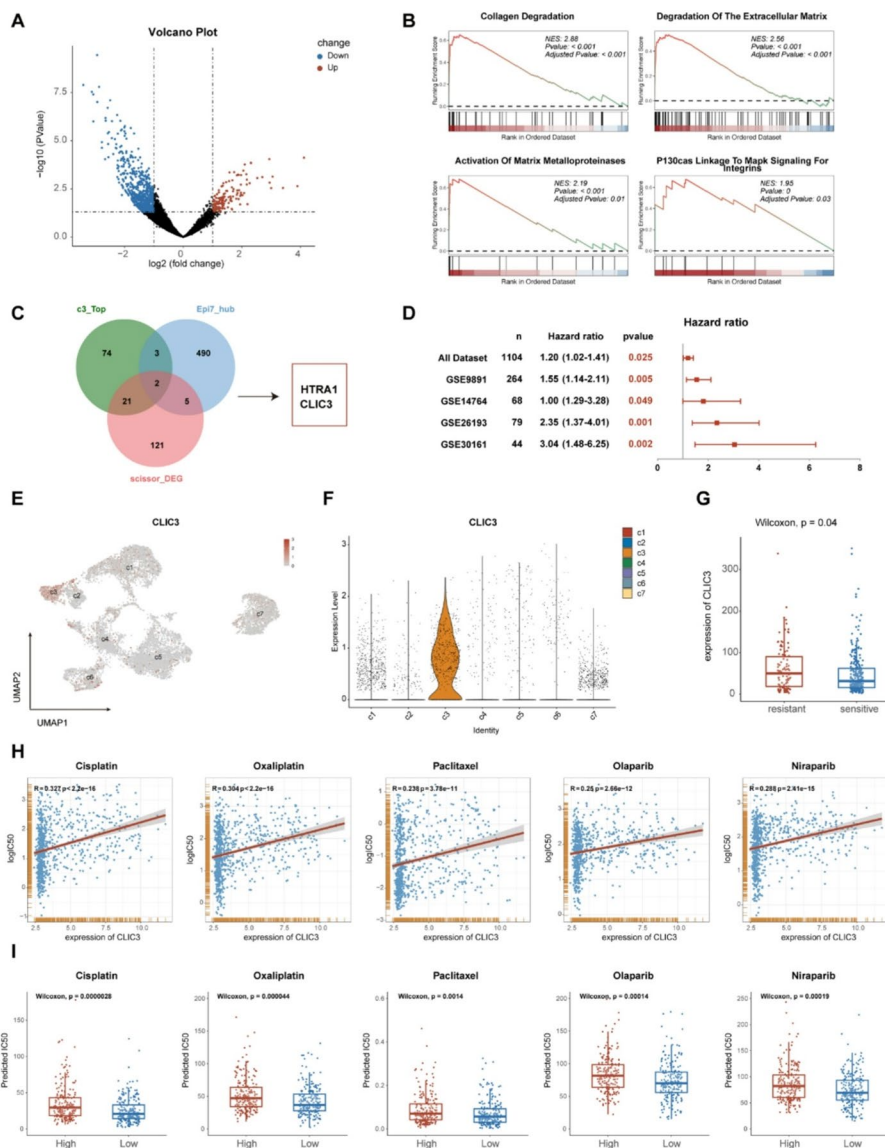


Fig. 5 CLIC3 is specifically expressed in the c3 subclusters and is associated with chemotherapy resistance in OC. A Volcano plot revealed the DEGs between scissor- and scissor+ cells. B GSEA analysis revealed pathways upregulated in the scissor+ cells. C Intersection of the top100 gene of c3, the hub genes of Epi7 and the upregulated genes in scissor+ cells. D Forest plot demonstrates the association between CLIC3 expression levels and PFS across multiple OC databases. E, F UMAP and violin plot showed the expression of CLIC3 among all epithelial cells. G The expression of CLIC3 between chemo-sensitive and resistant patients in TCGA cohorts. H Scatter plot showed the correlation between CLIC3 expression levels and the IC50 of various chemotherapy drugs in GDSC database. I The predicted IC50 of chemotherapy drugs between CLIC3 high-expression and low-expression group in TCGA cohorts

identified as being associated with chemoresistance (Fig. 5E, F). The expression levels of CLIC3 in the TCGA database also revealed a significant upregulation in chemo-resistant patients, suggesting that this gene plays a crucial role in chemoresistance in OC (Fig. 5G). Subsequently, we investigated the association between CLIC3 expression and the sensitivity to conventional chemotherapy agents (such as cisplatin, oxaliplatin, and paclitaxel) and PARP inhibitors (like Olaparib and niraparib), using data from the Genomics of Drug Sensitivity in Cancer (GDSC) database. The results showed that the IC50 of these drugs is positively correlated with CLIC3 expression (Fig. 5H). Additionally, using

the ‘oncoPredict’ R packages, we predicted the IC50 for the aforementioned drugs in TCGA samples and found the predicted IC50 of these drugs was higher in the CLIC3 high-expression group (Fig. 5I), which further indicates that our findings may contribute to the development of new therapeutic strategies for OC patients.

3.6 Investigation into the chemoresistance mechanisms of CLIC3

First, we analyzed the expression levels of CLIC3 across 33 types of tumors in the TCGA database and found that CLIC3 is significantly upregulated in various tumors, including bladder cancer, lung adenocarcinoma, ovarian cancer (Fig. 6A). Next, we analyzed the associations between CLIC3 expression and the enrichment scores of TCGA patients, derived from REACTOME and GOBP pathway analyses (Fig. 6B, C). CLIC3 negatively correlated with cell cycle and DNA repair pathways such as ‘GO cell cycle checkpoint’

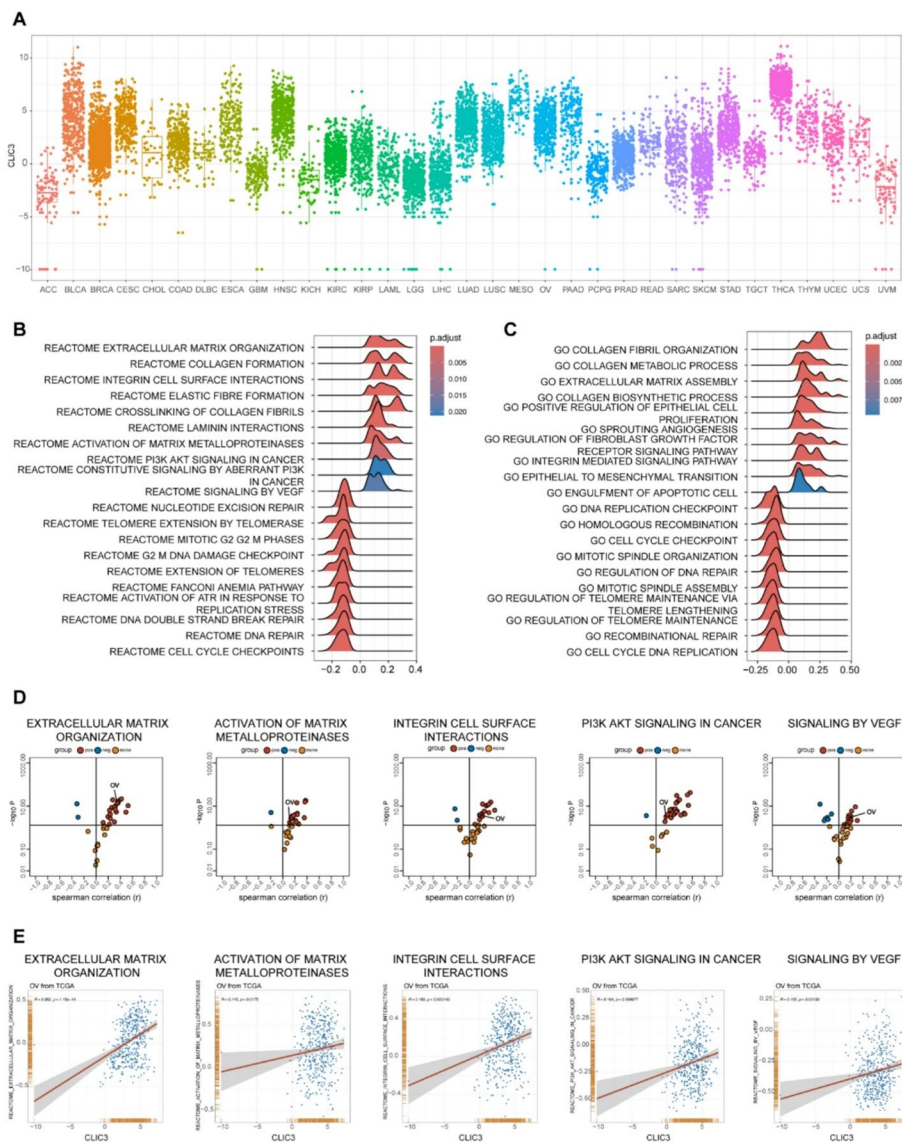


Fig. 6 CLIC3 promotes extracellular matrix formation by regulating integrins. A The expression levels of CLIC3 across 33 tumor types in the TCGA dataset. B, C REACTOME and GO pathways of CLIC3 determined by GSVA in TCGA database. D The correlation between CLIC3 expression and various pathways across 33 tumor types in the TCGA database. E Scatter plot showed the correlation between CLIC3 expression and various pathways in OC

and 'REACTOME DNA repair'. Furthermore, CLIC3 positively correlated to formation of ECM, integrin and VEGF pathways such as 'extracellular matrix organization', 'integrin cell surface interactions' and 'signaling by VEGF'. Finally, we examined the correlation between the expression of CLIC3 and these key pathways across 33 tumor types in the TCGA database. The results showed a positive correlation in most tumors, including OC (Fig. 6D, E). In summary, CLIC3 might promote chemoresistance through promoting integrin regulation, ECM formation and angiogenesis.

3.7 Downregulation of CLIC3 increases OC sensitivity to cisplatin by inhibiting integrin redistribution and PI3K-AKT pathway

To verify the function of CLIC3 in OC, we established a CLIC3-knockdown OC cell model. Western blot showed that CLIC3 was efficiently knocked down by Si-CLIC3#1, Si-CLIC3#2 and Si-CLIC3#3 (Fig. 7A). To gain deeper mechanistic insights into the relationship between intracellular CLIC3 expression levels and chemotherapeutic drug sensitivity, we assessed the cisplatin sensitivity of CLIC3-knockdown cell lines. Both Cell Counting Kit-8 (CCK-8) assays and sphere formation assays demonstrated that CLIC3 knockdown significantly enhanced cisplatin sensitivity in SKOV3 cells (Fig. 7B, C).

Previous bioinformatic analyses demonstrated a robust association between CLIC3 and integrin regulatory pathways, corroborating prior findings. Immunofluorescence staining showed that integrin $\beta 1$ less co-localized with DiO (cell membrane) in CLIC3-knockdown SKOV3 cells (Fig. 7D). Clinical samples confirmed CLIC3 expression was considerably higher in tumors from chemo-resistant patients than that in tumors from chemo-sensitive patients (Fig. 7E). More importantly, the tumor from chemo-resistant patients exhibited increased co-localization of integrin $\beta 1$ and CLIC3 (Fig. 7F).

Previous pathway enrichment analysis revealed that elevated CLIC3 expression was significantly associated with PI3K/AKT signaling pathway activation in OC. To investigate whether CLIC3 mediates this activation through integrin expression modulation, we then assessed protein level of integrin $\beta 1$, PI3K, AKT and pAKT in CLIC3-knockdown SKOV3 cells with cisplatin treatment and found increased level of integrin $\beta 1$, PI3K and pAKT/AKT compared with control cells, while CLIC3 depletion inhibited cisplatin-induced increasement of those protein expression (Fig. 7G). Taken together, our study demonstrates the cisplatin-induced changes of integrin $\beta 1$ expression and redistribution and promoting PI3K-AKT pathways, which is inhibited by the depletion of CLIC3.

4 Discussion

OC ranks among the top three malignancies in incidence and mortality within the female reproductive system, posing a significant global healthcare burden [1]. Due to its insidious onset and propensity for peritoneal metastasis, most OC patients are diagnosed at an advanced stage with widespread metastases. Standard treatment typically involves surgical resection followed by adjuvant chemotherapy. Platinum-based chemotherapy has significantly improved patient outcomes over the decades. Unfortunately, approximately two-thirds of the patients develop resistance to platinum, substantially increasing the five-year mortality rate [19]. Therefore, overcoming platinum resistance in OC patients is an urgent challenge.

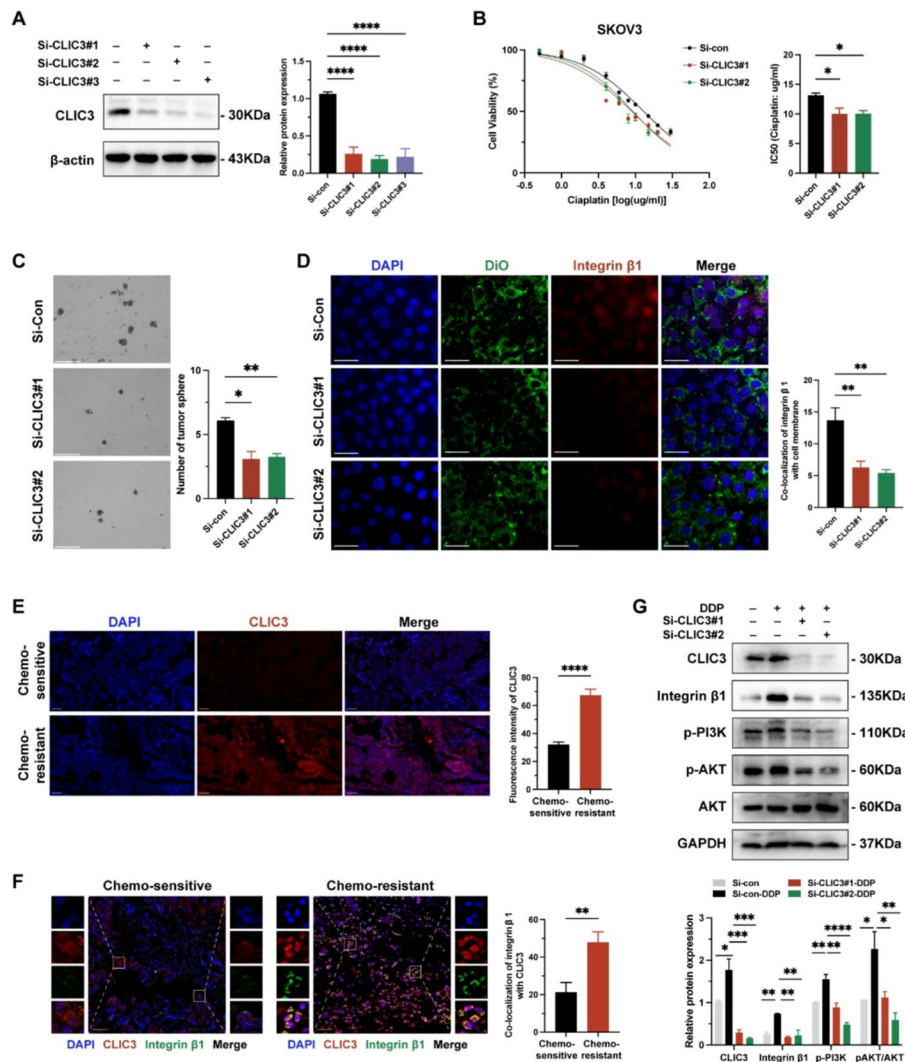


Fig. 7 Downregulation of CLIC3 increases OC sensitivity to cisplatin by inhibiting integrin redistribution and PI3K-AKT pathway. **A** Western blot indicating a significant decrease in CLIC3 protein levels following si-CLIC3 transfection (#1 and #2). **B** Cell viability of SKOV3 cell with CLIC3 depletion following dose-gradient cisplatin exposure. **C** Sphere formation assay was carried out using SKOV3 cell with CLIC3 depletion following cisplatin treatment. **D** SKOV3 cell was subjected to immunofluorescence staining for DiO (cell membrane, green), Integrin β1 (red) and 4',6-diamidino-2-phenylindole (DAPI, blue) following si-CLIC3 transfection. Representative images are shown in left [scale bars, 55 μm] and co-localization of Integrin β1 and cell membrane is displayed in right. **E** Left, representative images of CLIC3 (red) expression in ovarian tumor sample from patients from chemo-sensitive and chemo-resistant. Scale bars, 55 μm. Right, fluorescence intensity of CLIC3 (n = 10, t-test). **F** Left, co-localization of Integrin β1 (green) and CLIC3 (red) in OC specimens from a chemo-sensitive and chemo-resistant patient. Scale bars, 55 μm. Right, the percentage of Integrin β1 co-localized with CLIC3 (n = 10, t-test). **G** Expression of CLIC3, integrin β1, p-PI3K and AKT/pAKT in SKOV3 cell with CLIC3 depletion and cisplatin treatment. Data were presented as mean ± SEM. *p < 0.05, **p < 0.01, ***p < 0.001, ****p < 0.0001 for Student's t-test and one-way ANOVA test

In recent years, research on the mechanisms of platinum resistance in OC has surged, focusing primarily on drug efflux and the activation of DNA repair pathways [3]. However, due to significant inter-patient and intra-tumor heterogeneity, traditional methods such as tissue immunohistochemistry, fluorescence, and bulk transcriptome sequencing often obscure the underlying mechanisms of proliferation, metastasis, recurrence, and resistance in OC. The high resolution offered by 10X single-cell sequencing technology

significantly addresses these limitations, providing new hope for the treatment of OC patients [20].

We analyzed single-cell sequencing data from five OC samples in public databases, including three chemotherapy-resistant and two chemotherapy-sensitive samples. We observed a marked decrease in immune cells (B cells, T cells) in resistant tissues compared to sensitive samples, while epithelial-derived cells showed a significant increase. This aligns with the understanding that OC primarily originates from epithelial cells, which exert malignant functions, and that immune evasion facilitates cancer cell proliferation, metastasis, and recurrence [21]. Consequently, we further subclustered the epithelial cells based on gene expression patterns and associated biological functions.

We utilized the TCGA and GSE30161 OC cohorts to explore clinical characteristics and prognostic information associated with each epithelial subcluster. We identified a subcluster, c3, that was consistently linked to chemotherapy response and poor prognosis in both databases. Subsequent ligand-receptor interaction analysis revealed that the c3 subcluster had the most extensive communication with the tumor microenvironment, including fibroblasts, endothelial cells, and myeloid cells. Pathways such as VEGF, laminin, and collagen significantly contributed to this interaction. The VEGF pathway is intimately linked to angiogenesis [22] while laminin and collagen pathways are related to ECM remodeling, as tumor cells form ECM to hinder the approach of chemotherapeutic agents [18, 23, 24]. These findings align with our previous results indicating that c3 primarily participates in ECM formation. Therefore, it is proposed that the malignant cells in cluster 3 are the primary drivers of tumor resistance.

We further explored the gene modules in c3 and identified its hub genes named HTRA1 (HtrA Serine Peptidase 1) and CLIC3 (Chloride Intracellular Channel 3). To explore the functions of these two genes, we found that HTRA1 primarily involved in the development of age-related macular degeneration (AMD) [25, 26] while CLIC3 regulates the ECM through integrins and metalloproteinases [8, 9, 27–29]. Therefore, we shifted our focus to CLIC3. Although the role of CLIC3 in chemotherapy resistance is not extensively studied, its mechanisms involving ECM and tumor metastasis are well understood. Dozynkiewicz et al. (2012) first discovered that CLIC3 can redirect integrin $\alpha 5\beta 1$, recruited by RAB25 to lysosomes, back to the cell membrane to regulate ECM formation [8]. In the same year, Knowles et al. revealed that in bladder cancer, CLIC3 can induce autophagy through integrin $\alpha 5\beta 1$ ²⁷. Tringali et al.'s study in the same year demonstrated that CLIC3 influences integrin $\beta 1$ distribution, activating the EGFR and PI3K-AKT pathways to increase autophagy and reduce apoptosis, thereby contributing to bladder cancer resistance [9]. In 2014, Macpherson et al. found a new mechanism by which CLIC3 regulates the ECM in breast cancer, differing from Dev's 2012 findings, by proposing that CLIC3 can transport the metalloproteinase MMP14 extracellularly to modulate the ECM [29]. Similarly, Hernandez-Fernaud's 2017 study in breast cancer identified CLIC3 as a glutathione-dependent reductase that regulates ECM stiffness by modulating transglutaminase-2 (TGM2) activity [28].

However, the relationship between CLIC3 and chemotherapy resistance in OC has not yet been reported. Here, we have identified for the first time a subcluster of OC epithelial cells that specifically express CLIC3. Consistent with previous reports, biological function analysis and cell communication analysis of this subcluster indicate a close interaction with the tumor microenvironment. More importantly, clinical validation

revealed that these cells are closely associated with chemotherapy resistance and poor prognosis in OC. Functional analysis of CLIC3 showed that it primarily participates in ECM regulatory pathways, such as “extracellular matrix organization” and “extracellular matrix assembly,” further confirming that CLIC3 is a key gene in the functional execution of the c3 subcluster. Interestingly, we found that CLIC3 is involved in integrin regulatory pathways, including “integrin cell surface interactions” and “integrin mediated signaling pathway”. These pathways were also significantly enriched in our previous ligand-receptor interaction analysis and in the upregulated pathways of scissor+ cells. This is consistent with literature reports that CLIC3 can participate in tumor metastasis and resistance through various mechanisms involving integrins, including $\alpha5\beta1$ and $\beta1$.

To further substantiate the relationship between CLIC3 and chemotherapy resistance, we analyzed the expression levels of CLIC3 and the IC50 values of five standard OC chemotherapeutic agents, including cisplatin, oxaliplatin, paclitaxel, using the GDSC database across 809 cell lines. The results demonstrated a positive correlation between CLIC3 expression and the IC50 of these drugs. Similarly, analysis of the TCGA OC database indicated that patients with high CLIC3 expression are more likely to develop resistance to these chemotherapeutic agents. Mechanistically, we discovered that CLIC3 actively participates in pathways involving ECM formation, integrin regulation, and angiogenesis across various tumors, including OC.

In our study, consistent with bioinformatics analysis, demonstrate that depletion of CLIC3 significantly increases the sensitivity of SKOV3 cells to cisplatin. Previous studies have established that RAD25 facilitates integrin translocation to lysosomes for degradation, whereas CLIC3 orchestrates retrograde transport of integrins from lysosomes to the plasma membrane to avert clearance [8]. Constantly with previous hypothesis, our data demonstrate that CLIC3 knockdown significantly reduces integrin $\beta1$ expression and impairs plasma membrane localization. Importantly, in the chemo-resistant samples, we observed a significant increase in the co-localization levels of CLIC3 and integrin $\beta1$ compared to the sensitive samples. Furthermore, we validated CLIC3 depletion inhibited cisplatin-induced activation of the PI3K-AKT pathways. Thus, our study shows that CLIC3-dependent redistribution of integrin $\beta1$ on the cell membrane, resulting the activation of the PI3K-AKT pathways, thus providing a mechanistic basis for platinum resistant. However, the specific mechanisms through which CLIC3 regulates integrin expression and membrane localization remain unexplored in this study. We therefore plan to undertake more detailed investigations to elucidate these regulatory mechanisms and validate them comprehensively through in vivo experiments.

5 Conclusion

This study offers a novel insight into the progression and chemoresistance of ovarian cancer (OC). Additionally, we identified a specific cell cluster highly associated with chemoresistance. The marker for this cluster, CLIC3, increases OC resistance to cisplatin by promoting integrin $\beta1$ redistribution and PI3K-AKT pathway and holds significant potential as a new therapeutic target for OC.

Supplementary Information

The online version contains supplementary material available at <https://doi.org/10.1007/s12672-025-02882-9>.

Supplementary Material 1 Figure S1 A UMAP of integrated data identified 26 cell clusters. B Dot plot showed the

markers of each cell clusters.

Supplementary Material 2 FigureS2 UMAP and violin plot showed ECM-related pathways in epithelial cell subclusters.

Supplementary Material 3 Figure S3 Kaplan–Meier analysis for patients from TCGA cohort with high and low GSVA score based on the top markers of 7 cell subclusters.

Supplementary Material 4 FigureS4 A Kaplan–Meier analysis for patients from GSE30161 cohort with high and low GSVA score based on the top markers of 7 cell subclusters. B GSVA score based on the top markers of 7 cell subclusters between chemo-sensitive and resistant OC patients in GSE30161 cohorts.

Supplementary Material 5

Supplementary Material 6

Supplementary Material 7

Acknowledgements

We would like to thank Jianming Zeng (University of Macau) and all members of his bioinformatics team, biotraine, for generously sharing their experience and codes.

Author contributions

ZFL and XTZ conceived and designed the study. ZFL wrote the manuscript. ZFL and JL participated in bioinformatics analysis. YL, JJY supported the study. WTY supervised the study. XTZ and WTY revised the manuscript. All authors read and approved the final manuscript.

Funding

This work was supported by grants from the National Natural Science Foundation of China (Grant/Award No. 82373397), the Capital's Funds for Health Improvement and Research (Grant/Award No.2022-2-2116) and Laboratory for Clinical Medicine, Capital Medical University.

Data availability

The code used in our study can be obtained from the corresponding author. The data sets used in the present research were summarized in the Additional file 5: Table S1.

Declarations

Competing interests

The authors declare no competing interests.

Received: 22 January 2025 / Accepted: 2 June 2025

Published online: 14 June 2025

References

1. Bray F, Laversanne M, Sung H, et al. Global cancer statistics 2022: GLOBOCAN estimates of incidence and mortality worldwide for 36 cancers in 185 countries. *CA Cancer J Clin.* 2024;74(3):229–63. <https://doi.org/10.3322/caac.21834>.
2. Richardson DL, Eskander RN, O'Malley DM. Advances in ovarian Cancer care and unmet treatment needs for patients with platinum resistance: A narrative review. *JAMA Oncol.* 2023;9(6):851–9. <https://doi.org/10.1001/jamaoncol.2023.0197>.
3. Rottenberg S, Disler C, Perego P. The rediscovery of platinum-based cancer therapy. *Nat Rev Cancer.* 2021;21(1):37–50. <https://doi.org/10.1038/s41568-020-00308-y>.
4. Prakash J, Shaked Y. The interplay between extracellular matrix remodeling and Cancer therapeutics. *Cancer Discov.* 2024;14(8):1375–88. <https://doi.org/10.1158/2159-8290.CD-24-0002>.
5. Darvishi B, Eisavand MR, Majidzadeh-A K, Farahmand L. Matrix stiffening and acquired resistance to chemotherapy: concepts and clinical significance. *Br J Cancer.* 2022;126(9):1253–63. <https://doi.org/10.1038/s41416-021-01680-8>.
6. Norman J, Zanivan S. Chloride intracellular channel 3: A secreted pro-invasive oxidoreductase. *Cell Cycle.* 2017;16(21):1993. <https://doi.org/10.1080/15384101.2017.1377031>.
7. Shuai Y, Zhang H, Liu C, et al. CLIC3 interacts with NAT10 to inhibit N4-acetylcytidine modification of p21 mRNA and promote bladder cancer progression. *Cell Death Dis.* 2024;15(1):9. <https://doi.org/10.1038/s41419-023-06373-z>.
8. Dozynkiewicz MA, Jamieson NB, MacPherson I, et al. Rab25 and CLIC3 collaborate to promote integrin recycling from late endosomes/lysosomes and drive Cancer progression. *Dev Cell.* 2012;22(1):131. <https://doi.org/10.1016/j.devcel.2011.11.008>.
9. Tringali C, Lupo B, Silvestri I, et al. The plasma membrane Sialidase NEU3 regulates the malignancy of renal carcinoma cells by controlling β 1 integrin internalization and recycling. *J Biol Chem.* 2012;287(51):42835. <https://doi.org/10.1074/jbc.M112.407718>.
10. Clough E, Barrett T. The gene expression omnibus database. *Methods Mol Biol.* 2016;1418:93–110. https://doi.org/10.1007/978-1-4939-3578-9_5.
11. Goldman MJ, Craft B, Hastie M, et al. Visualizing and interpreting cancer genomics data via the Xena platform. *Nat Biotechnol.* 2020;38(6):675–8. <https://doi.org/10.1038/s41587-020-0546-8>.
12. Wu T, Hu E, Xu S, et al. ClusterProfiler 4.0: A universal enrichment tool for interpreting omics data. *Innov (Camb).* 2021;2(3):100141. <https://doi.org/10.1016/j.xinn.2021.100141>.
13. Hänzelmann S, Castelo R, Guinney J. GSVA: gene set variation analysis for microarray and RNA-seq data. *BMC Bioinform.* 2013;14:7. <https://doi.org/10.1186/1471-2105-14-7>.

14. Sun D, Guan X, Moran AE, et al. Identifying phenotype-associated subpopulations by integrating bulk and single-cell sequencing data. *Nat Biotechnol.* 2022;40(4):527–38. <https://doi.org/10.1038/s41587-021-01091-3>.
15. Jin S, Guerrero-Juarez CF, Zhang L, et al. Inference and analysis of cell-cell communication using cellchat. *Nat Commun.* 2021;12(1):1088. <https://doi.org/10.1038/s41467-021-21246-9>.
16. Guo J, Han X, Li J, et al. Single-cell transcriptomics in ovarian cancer identify a metastasis-associated cell cluster overexpressed RAB13. *J Transl Med.* 2023;21(1):254. <https://doi.org/10.1186/s12967-023-04094-7>.
17. Li J, Li Z, Gao Y, et al. Integrating single-cell RNA sequencing and prognostic model revealed the carcinogenicity and clinical significance of FAM83D in ovarian cancer. *Front Oncol.* 2022;12:1055648. <https://doi.org/10.3389/ponc.2022.1055648>.
18. Pietilä EA, Gonzalez-Molina J, Moyano-Galceran L, et al. Co-evolution of matrisome and adaptive adhesion dynamics drives ovarian cancer chemoresistance. *Nat Commun.* 2021;12(1):3904. <https://doi.org/10.1038/s41467-021-24009-8>.
19. Vaughan S, Coward JI, Bast RC, et al. Rethinking ovarian cancer: recommendations for improving outcomes. *Nat Rev Cancer.* 2011;11(10):719–25. <https://doi.org/10.1038/nrc3144>.
20. Gohil SH, Iorgulescu JB, Braun DA, Keskin DB, Livak KJ. Applying high-dimensional single-cell technologies to the analysis of cancer immunotherapy. *Nat Reviews Clin Oncol.* 2020;18(4):244. <https://doi.org/10.1038/s41571-020-00449-x>.
21. Moufarrij S, Dandapani M, Arthofer E, et al. Epigenetic therapy for ovarian cancer: promise and progress. *Clin Epigenetics.* 2019;11(1):7. <https://doi.org/10.1186/s13148-018-0602-0>.
22. Cao Y, Langer R, Ferrara N. Targeting angiogenesis in oncology, ophthalmology and beyond. *Nat Rev Drug Discov.* 2023;22(6):476–95. <https://doi.org/10.1038/s41573-023-00671-z>.
23. Kalluri R. The biology and function of fibroblasts in cancer. *Nat Rev Cancer.* 2016;16(9):582–98. <https://doi.org/10.1038/nrc.2016.73>.
24. Chen X, Song E. Turning foes to friends: targeting cancer-associated fibroblasts. *Nat Rev Drug Discov.* 2019;18(2):99–115. <https://doi.org/10.1038/s41573-018-0004-1>.
25. Gerhardy S, Ultsch M, Tang W, et al. Allosteric Inhibition of HTRA1 activity by a conformational lock mechanism to treat age-related macular degeneration. *Nat Commun.* 2022;13:5222. <https://doi.org/10.1038/s41467-022-32760-9>.
26. Pan Y, Fu Y, Baird PN, Guymer RH, Das T, Iwata T. Exploring the contribution of ARMS2 and HTRA1 genetic risk factors in age-related macular degeneration. *Prog Retin Eye Res.* 2023;97:101159. <https://doi.org/10.1016/j.preteyeres.2022.101159>.
27. Knowles LM, Zewe J, Malik G, Parwani AV, Gingrich JR, Pilch J. CLT1 targets bladder Cancer through integrin $\alpha 5 \beta 1$ and CLIC3. *Mol Cancer Res: MCR.* 2012;11(2):194. <https://doi.org/10.1158/1541-7786.MCR-12-0300>.
28. Hernandez-Fernaund JR, Ruengeler E, Casazza A, et al. Secreted CLIC3 drives cancer progression through its glutathione-dependent oxidoreductase activity. *Nat Commun.* 2017;8:14206. <https://doi.org/10.1038/ncomms14206>.
29. Macpherson IR, Rainero E, Mitchell LE, et al. CLIC3 controls recycling of late endosomal MT1-MMP and dictates invasion and metastasis in breast cancer. *J Cell Sci.* 2014;127(18):3893–901. <https://doi.org/10.1242/jcs.135947>.

Publisher's note

Springer Nature remains neutral with regard to jurisdictional claims in published maps and institutional affiliations.